COBEM 2023 27TH INTERNATIONAL CONGRESS OF MECHANICAL ENGENEERING

ABCM Brazilian Society of Mechanical Sciences and Engineering
27th ABCM International Congress of Mechanical Engineering
December 04-08, 2023, Florianópolis-SC, Brazil

COB-2023-0865
STRATEGIES TO EVALUATE THE RESULTS OF A CFD-BASED SOLUTION TO INVESTIGATE THE AEROELASTIC DYNAMICS OF A TYPICAL SECTION AIRFOIL

Bianca Taís Visoná Carnielo
Aluisio Viais Pantaleão
Douglas D. Bueno
São Paulo State University (UNESP) - Av. Brasil, 56 - Centro - Ilha Solteira/SP
bianca.carnielo@unesp.br, aluisio.pantaleao@unesp.br, douglas.bueno@unesp.br

Abstract. *Aeroelasticity is the branch which comprises studies involving interactions between structural and aerodynamic forces, mainly focusing on aerial vehicles. The fluid-structure interactions (FSI) solution can be achieved by coupling the CFD and the Finite Element Method (FEM) for structural analysis. The present work comprises aeroelastic simulations considering a two dimensional airfoil NACA 0012 with two degrees of freedom. Different subsonic flow conditions are considered to investigate the airfoil with pitch and plunge motions, and to map the airfoil until achieving the unstable motion. The structural mesh is developed by using the Finite Element Method through the software Nastran. The solution uses the open-source software SU2 supported by the SU2 Foundation. Different aspects involving the obtained dynamics are investigated, including the stagnation point over time, the lift force and the aerodynamic pitch moment. The magnitude of the lift force is obtained by considering the mean pressure between two adjacent grid points and the distance between them, the direction of the lift force vector is obtained considering the decomposition of the force normal to the airfoil surface in the vertical direction. The pressure and velocity fields are also investigated. The results demonstrate that the airfoil is stable until Mach 0.52, and that the used procedure is efficient to provide the solution of this type of FSI problem.*

Keywords: *SU2, Fluid-structure interaction, CFD, Aeroelasticity.*

1. INTRODUCTION

Aeroelasticity is a science focused on studying the mutual interaction between aerodynamic forces and elastic forces, and the influence of their interaction on the airplane design. It is a topic on the field of FSI (Fluid Structure Interaction) problems Modern airplane structures are very flexible, and this flexibility contributes to be verified various types of aeroelastic problems (Bisplinghoff *et al.*, 1996).

This interaction of a flexible structure with a flowing fluid in which it is immersed gives rise to a variety of physical phenomena such as flutter, responses to buffeting loads, limit cycle oscillations, and others. These phenomena can be investigated by using dynamic model for both structure and fluid (Dowell and Hall, 2001). Once it must be light, an airplane deforms due to the load, these deformations change the distribution of the aerodynamic forces, which in turn changes the deformations (Garrick and Reed, 1981).

Fluid structure interaction techniques have been widely used in many industrial problems for aerospace applications. It is performed aeroelastic computations by means of a coupled approach with these techniques where the aerodynamic forces are computed from the solution of the Navier-Stokes equations (Guerri *et al.*, 2008). The solution of Navier-Stokes equations is developed by Computational Fluid Dynamics (CFD), that is a branch of fluid mechanics that uses numerical methods and computational algorithms to solve complex problems involving fluid flow (Dash, 2016). The use of CFD to investigate the aerodynamic behavior of an airfoil is common in literature (Şahin and Acir, 2015; Gunel *et al.*, 2016; Zaide and Raveh, 2006), and it is also used in aeroelastic problems as a tool of flutter prediction (Li *et al.*, 2021). Moreover, the structure dynamics of a FSI problem are commonly modeled by the Finite Element Method like in Koohi *et al.* (2014); Teixeira and Awruch (2005); Nikbay *et al.* (2009); Grisval and Liauzun (1999); Das and Roy (2018); Peruru and Abbisetti (2017), once in the analysis of complex structures, the Finite Element model can be reduced in size by first finding the natural or eigenmodes of the structure and then recasting the finite element structural model in terms of these modes. This reduces not only the size of the model but also the computational cost by orders of magnitude (Dowell and Hall, 2001).

In particular, solutions to FSI problems in aeronautics can be obtained using the free software SU2, created by the *SU2 Foundation*, and developed and maintained by Stanford University, USA (SU2 Foundation, 2022). The software has been used to solve several problems, including in the transonic regime, as shown by Economon *et al.* (2016) and Ryabinin and Kuzmin (2020). The FSI coupling approach employed in SU2 is described by Sanchez *et al.* (2016). The authors evaluate the software's ability to perform aeroelastic analysis using computational tools, and also employing communication with external computational code through a wrapper resource written in Python.

Fonzi *et al.* (2021) developed an update of the Python–based fluid structure interaction framework of SU2 code and extended it to allow efficient and fully open source simulations of aeroelastic phenomena. It was also introduced a native code to solve the structural equations coming from a Nastran–like Finite Element Model. In this sense, the present work comprises aeroelastic simulations applying the SU2 fluid structure interaction methodology.

The airfoil NACA 0012 with two degrees of freedom is considered. Different subsonic flow conditions are evaluated to investigate the airfoil with pitch and plunge motions in the subsonic flow in both time and frequency domains. An analysis of the aerodynamic forces is done for Mach numbers in stable and unstable conditions through a methodology developed to obtain the aerodynamic loads from the pressure data. The results show the aerodynamic force distribution on the airfoil surface, the lift force and the displacement of stagnation point over time.

2. METHODOLOGY

The aeroelastic system investigated in this article is the NACA 0012 airfoil with two degrees of freedom (DOF). They correspond to the pitch angle (α) and the plunge (h) DOFs, and the system is illustrated in Fig. 1. The numerical solution is obtained by employing the open source software SU2, which is supported by the SU2 Foundation. It allows one to couple the computational code developed to solve the fluid dynamics with an algorithm written in Python to solve the structural dynamics.

The aerodynamic model is based on the Unsteady Reynolds Averaged Navier-Stokes (URANS) equations, with Menter's k-ω Shear Stress Transport (SST) turbulence model (Menter, 1993, 1994). The fluid domain is discretized with 133000 nodes, and refined close to the airfoil surface to represent the turbulent boundary layer. The employed mesh was previously validated by Fonzi *et al.* (2021) for this type of analysis. The aerodynamic forces are obtained by the CFD solution and it is interpolated from the fluid mesh to the structural mesh. The interpolation process is performed by the RBF (Radial Basis Functions) method. The structural model is obtained by considering a single point placed at the rotation axis (i.e., the elastic center). It is the master node, and the airfoil inertia and mass properties are both considered concentrated at the center of mass of the profile. The Finite Element Method is employed to obtain the structural mesh, and it is obtained from the software Nastran, that computes the system's modes and frequencies. The time integration of the structural equations of motion is done by the α-generalized method.

The aeroelastic equation of motion is given by $\mathbf{M\ddot{u}} + \mathbf{Ku} = \mathbf{F}_a$, where $\mathbf{M}$ is the mass matrix, $\mathbf{u}$ is the displacement vector, $\mathbf{K}$ is the stiffness matrix and $\mathbf{F}_a$ is the vector of aerodynamic forces. This equation can be rewritten in the generalized coordinate system by using the change of coordinate matrix given by the system modes, i.e, $\mathbf{\Phi} = [\mathbf{\Phi}_y \;\; \mathbf{\Phi}_\theta]$, where $\mathbf{\Phi}_y$ and $\mathbf{\Phi}_\theta$ are the undamped structural modes respectively related to plunge and pitch DOFs. So the displacements vector is rewritten such that $\mathbf{u} \cong \mathbf{\Phi u}_\Phi$ and the equation of motion becomes $\mathbf{M\Phi\ddot{u}}_\Phi + \mathbf{K\Phi u}_\Phi = \mathbf{F}_a$, and pre-multiplying it by $\mathbf{\Phi}^T$, it is obtained $\mathbf{\Phi}^T\mathbf{M\Phi\ddot{u}}_\Phi + \mathbf{\Phi}^T\mathbf{K\Phi u}_\Phi = \mathbf{\Phi}^T\mathbf{F}_a$. Therefore, the equation of motion in the generalized coordinate system is given by the following equation

$$\mathbf{M}_\Phi\ddot{\mathbf{u}}_\Phi + \mathbf{K}_\Phi\mathbf{u}_\Phi = \mathbf{F}_{a\Phi} \tag{1}$$

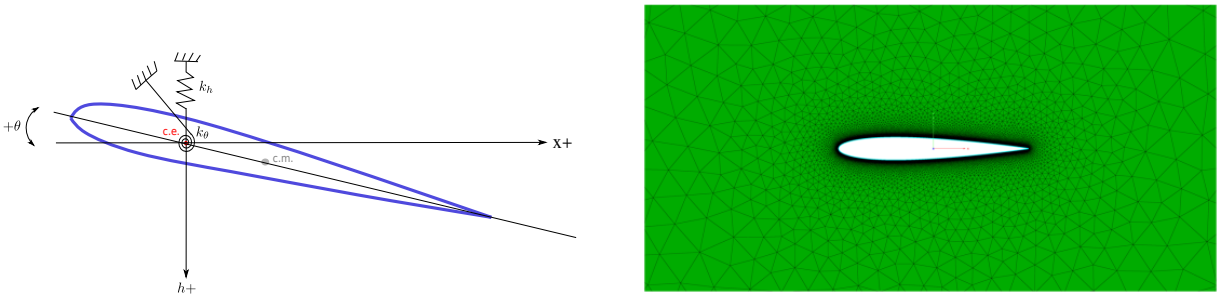

(a) Airfoil representative scheme (b) Fluid mesh

Figure 1. Airfoil with two degrees of freedom and fluid mesh.

The procedure to obtain the aerodynamic forces on the airfoil uses the aerodynamic pressure computed by SU2 and the airfoil contour geometry. First, the distances between two adjacent grid points are obtained, on the airfoil surface, such that

$$s_i = \sqrt{(x_{i+1} - x_i)^2 + (y_{i+1} - y_i)^2} \tag{2}$$

where s_i is the distance between the points (x_i, y_i) and (x_{i+1}, y_{i+1}) that matches the length of the i-th panel on the airfoil contour. The direction vector of the line formed by these two points is given by

$$\mathbf{s}_i = \{(x_{i+1} - x_i) \quad (y_{i+1} - y_i)\} \tag{3}$$

Note that it is assumed that the airfoil surface discretization is appropriate such that the segment between the two points is nearly a straight line. Then, the mean point of the panel is given by

$$P_i^{med} = \left(\frac{(x_{i+1} + x_i)}{2}, \frac{(y_{i+1} + y_i)}{2} \right) \tag{4}$$

It is possible to obtain the aerodynamic force, per span unit, by the product between the distance (s_i) and the mean aerodynamic pressure on the panel, in the mean point (P_i^{med}), such that

$$p_i = \frac{p_{(x_i,y_i)} + p_{(x_{i+1},y_{i+1})}}{2} \tag{5}$$

The direction of the aerodynamic force is normal to the panel, hence, it can be obtained by the vector product between the direction vector $\mathbf{s}_i$ and the unit vector $\hat{k} = \{0 \quad 0 \quad 1\}$, considering that the points are listed anticlockwise, such that $\mathbf{n}_i = \mathbf{s}_i \times \hat{k}$. Then, $\mathbf{F}_{a_i} = p_i s_i \mathbf{n}_i$ and, hence the magnitude of the aerodynamic force on the i-th panel is given by the norm of the vector $\mathbf{F}_{a_i} = \{F_{a_i}^x \quad F_{a_i}^y\}^T$, the lift force is the y compound of the aerodynamic force, such that the total lift force is given by

$$L = \sum_{i=1}^{N-1} F_{a_i}^y \tag{6}$$

where N is the total number of points around the airfoil and $F_{a_i}^y$ is the y compound of the aerodynamic force on the i-th panel. The Figure 2 shows a schematic illustration for two arbitrary the points and the corresponding vectors arrangement.

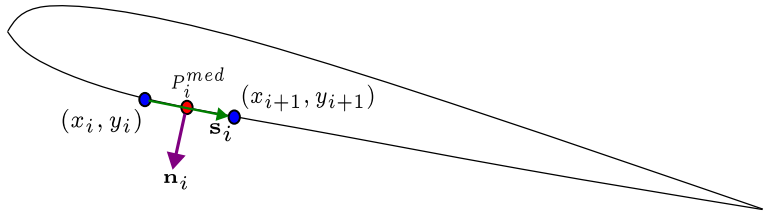

Figure 2. Representative scheme of the vectors and point arrangement.

3. RESULTS AND DISCUSSION

The numerical simulations were developed considering a Reynolds number of 4×10^6, the fluid domain consists of a circle with 100 chords of diameter that is discretized with 133000 nodes and refined close to the airfoil surface to represent the boundary layer. The Mach number was varied to map the airfoil stability. The structural mesh has 123 nodes that are connected to the master node by rigid bar elements, these elements do not include physical stiffness to the model, they just attach the nodes displacement to the master node displacement. Two spring elements are connected to the master node to represent the pitch and plunge stiffness. The physical and geometric parameters are shown in Tab. 1.

Table 1. Physical and geometric parameters of the structural model.

Parameter	Value
Mass	$81,35\ kg$
Inertia	$3,81\ kg.m^2$
Pitch stiffness	$16711,17\ N/m$
Plunge stiffness	$10295,99\ N/m$
Chord	$1\ m$
Pitch natural frequency	$8,38\ Hz$
Plunge natural frequency	$2,25\ Hz$

This section presents numerical results computed for different Mach numbers. The time histories for the pitch and plunge motions are shown in Fig. 3. The Fourier transform was used to compute the responses in the time domain and are shown in Fig. 4. The time histories show that the amplitudes rise over time for Mach 0.52, what does not happen for the other two Machs analyzed. Figure 4 shows that for pitch motion there is a change in frequency from Mach 0.38 to the others. The plunge motion frequencies remain about the same. Also, the amplitudes for Mach 0.52 are substantially higher. Because of the change in the pitch frequency, both modes present similar frequencies, and then the system becomes unstable, that is why the amplitudes rise with time for Mach number 0.52.

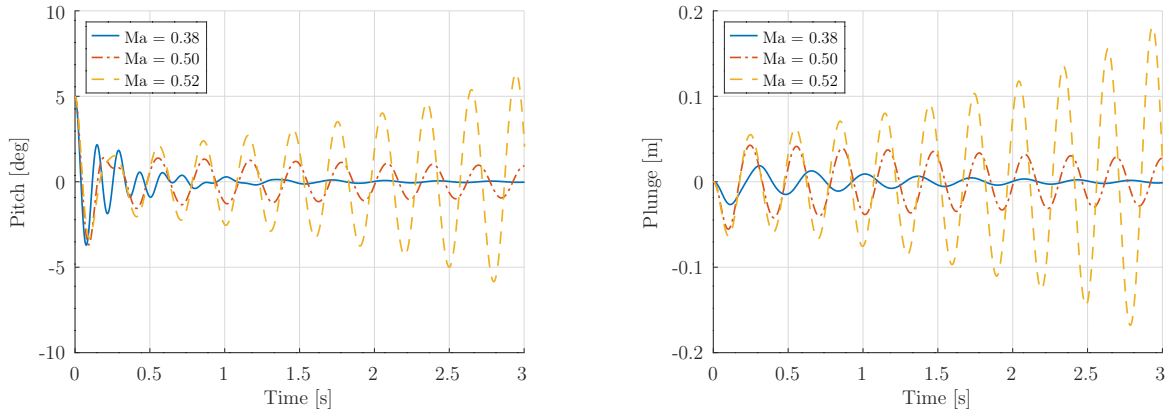

(a) Pitch (b) Plunge

Figure 3. Pitch and plunge motions over time.

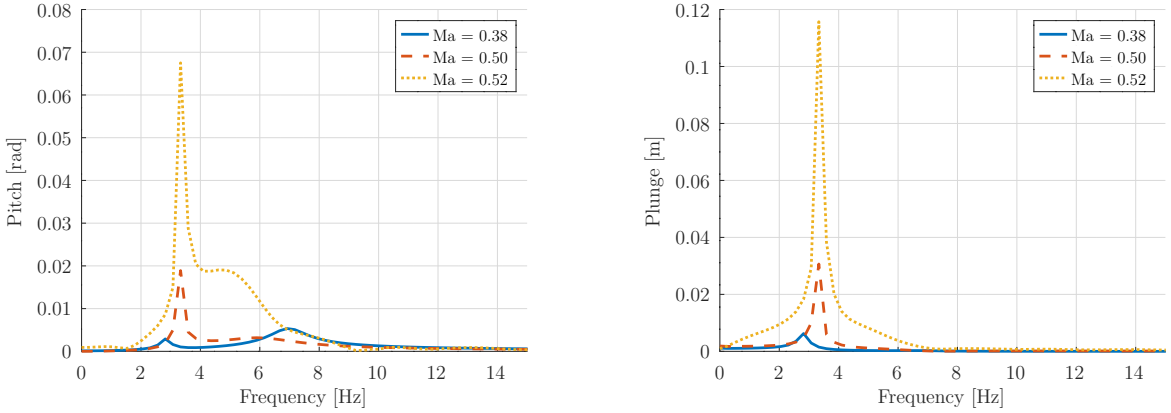

(a) Pitch (b) Plunge

Figure 4. Pitch and plunge frequencies.

The Mach numbers 0.38 (stable) and 0.52 (unstable) are analyzed in terms of aerodynamic forces by the methodology presented in Sec.2. Figure 5 shows a comparison between the lift force and the plunge motion normalized by its respective maximum value for both Mach numbers. Figure 6 shows the results for pitch motion and it shows that for both Mach numbers the lift force has similarities with the pitch motion. That is expected once, for a symmetrical airfoil, only there is lift force if there is an angle of attack (pitch motion). Note that the increasing amplitude over time indicates an aeroelastic instability and further investigations can be done to verify the Mach number corresponding to the flutter phenomenon

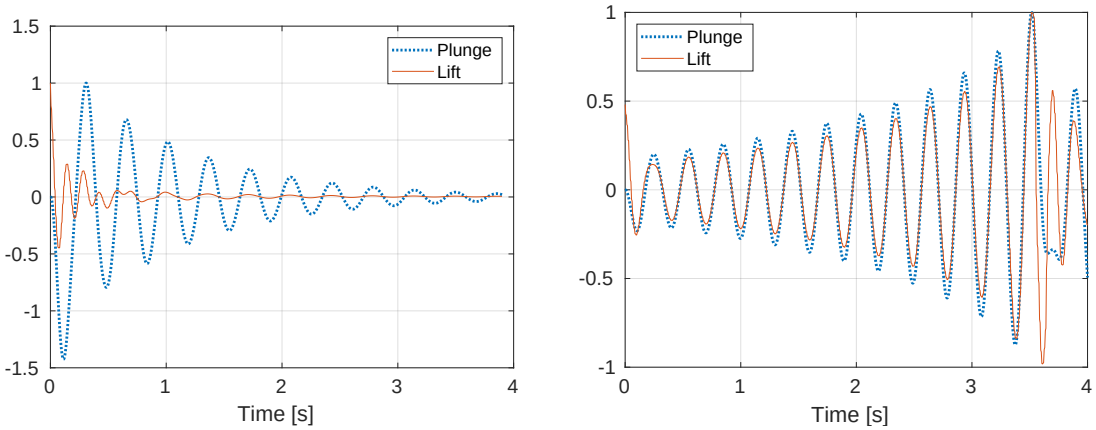

(a) Mach 0.38 (b) Mach 0.52

Figure 5. Lift force and plunge motion normalized by its respective maximum values.

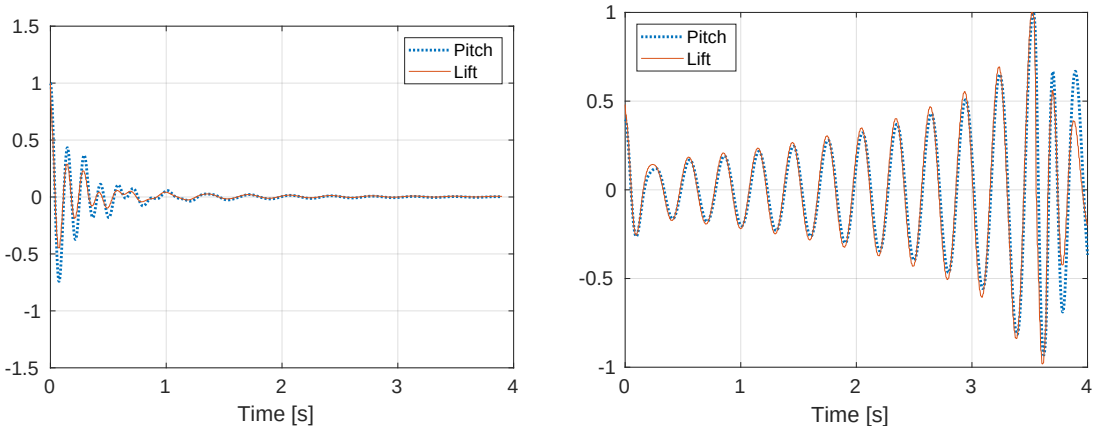

(a) Mach 0.38 (b) Mach 0.52

Figure 6. Lift force and pitch motion normalized by its respective maximum values.

The distribution of aerodynamic force on the airfoil surface allows one to determine the position of the stagnation point. It is the point in which the flow velocity is equal to zero, and typically it is near the leading edge of the airfoil. Figures 7 and 8 show the position of the stagnation point in x and y axis over time for Mach numbers 0.38 e 0.52, respectively. The position of the stagnation point in y axis has a behavior similar to the plunge motion for both cases.

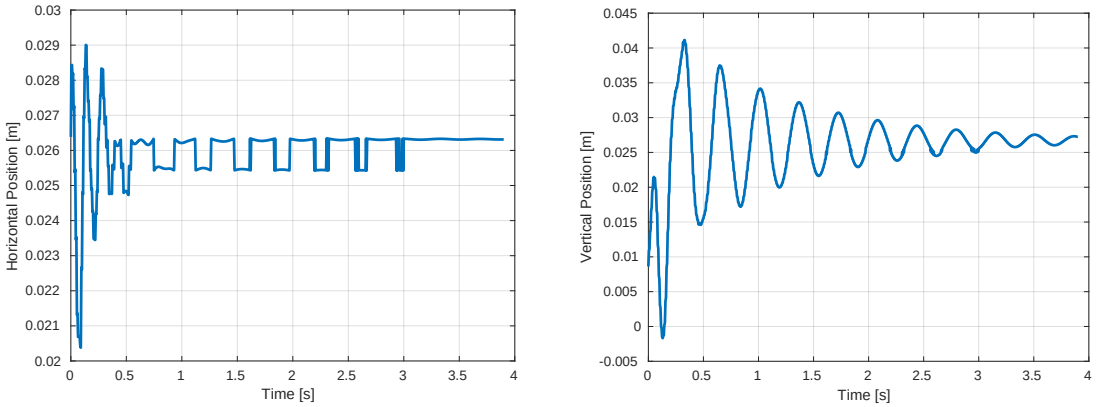

(a) Horizontal (b) Vertical

Figure 7. Stagnation point position over time for Mach 0.38.

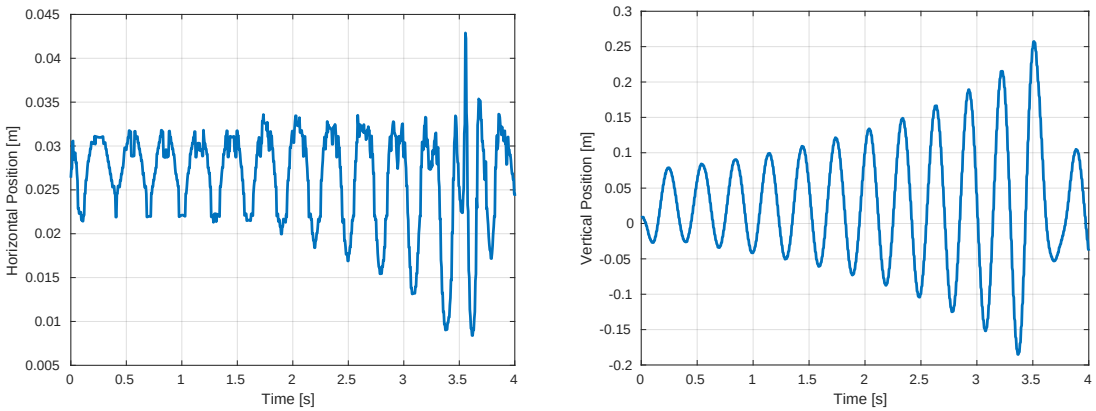

(a) Horizontal (b) Vertical

Figure 8. Stagnation point position over time for Mach 0.42.

Figures 9 and 10 show the distribution of aerodynamic force on the airfoil surface at different instants of time for Mach numbers 0.38 and 0.52, respectively. The figures show that the variation of force is minimal for Mach 0.38, and for Mach 0.52 there is a change in aerodynamic forces, position of the airfoil and position of stagnation point.

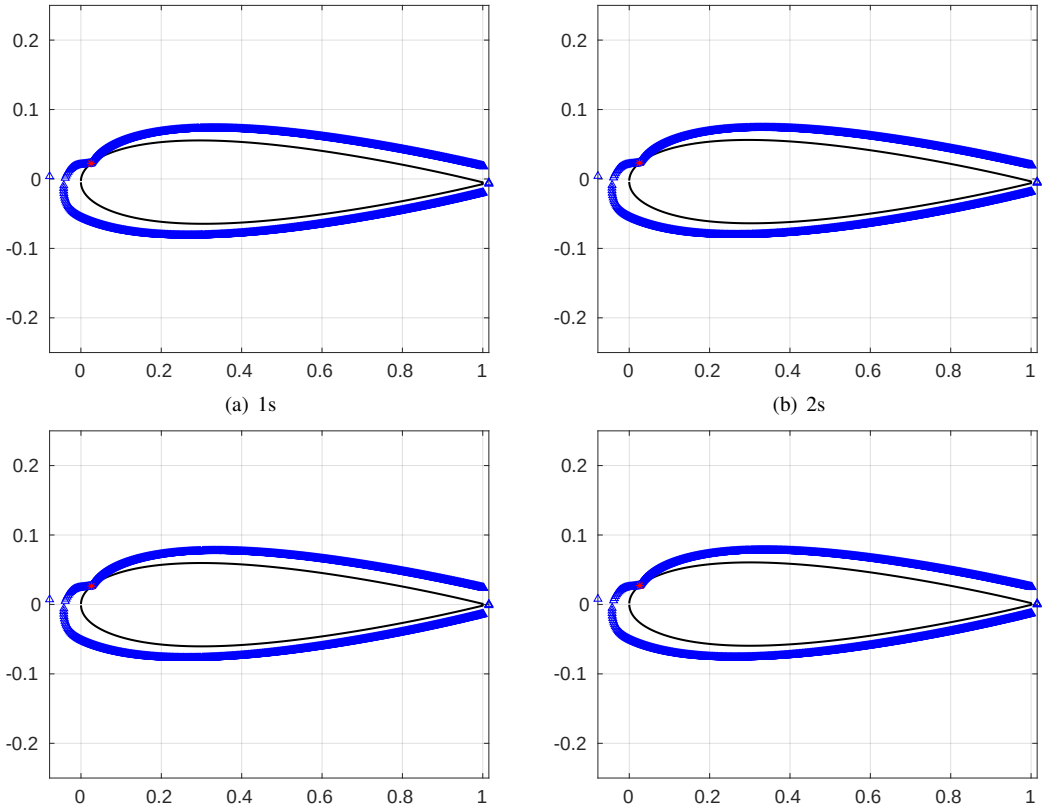

(a) 1s (b) 2s

(c) 3s (d) 4s

Figure 9. Aerodynamic force (blue) on the airfoil surface (black) and stagnation point (red) for Mach 0.38.

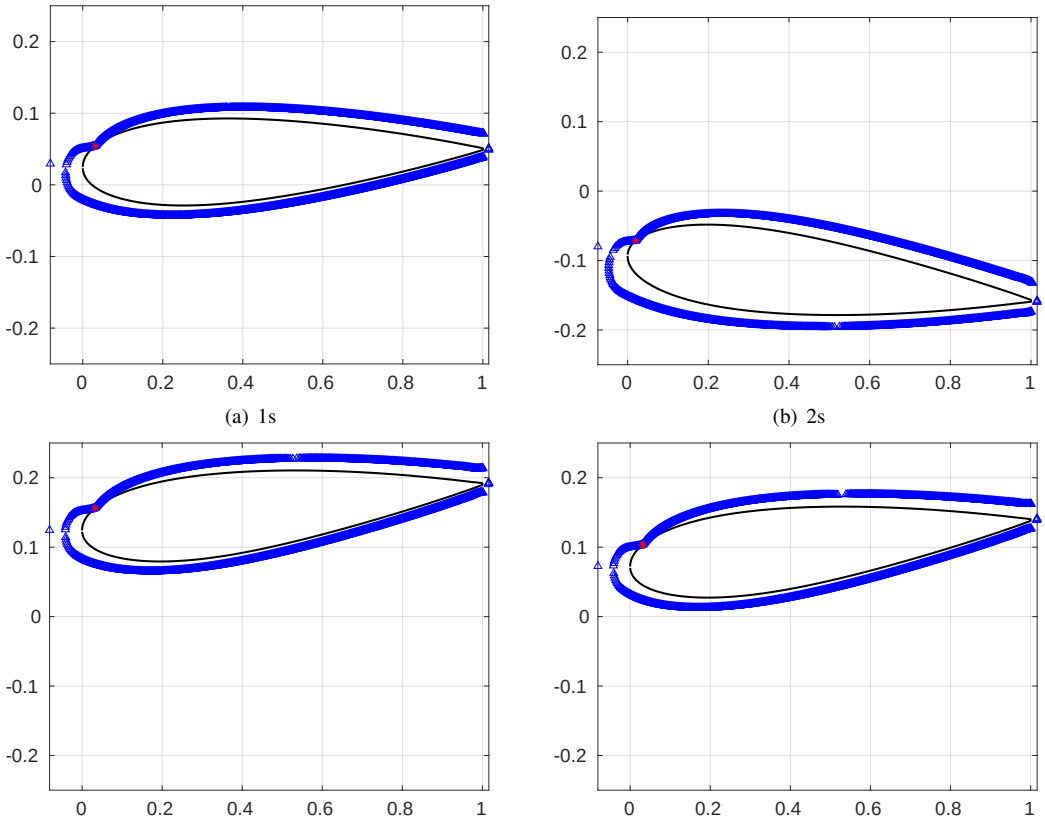

(a) 1s (b) 2s

(c) 3s (d) 4s

Figure 10. Aerodynamic force (blue) on the airfoil surface (black) and stagnation point (red) for Mach 0.52.

Figures 11 e 12 show the variation of lift force over time for Mach number 0.38 and 0.52, respectively. For the first one, note that the variation is small at the instants of time after $1s$, that is why the distributions of force in Fig. 9 are similar, this happens because the pitch displacements are about zero after $1s$. The lift variation frequencies are equal to $6.94Hz$ for Mach 0.38, and $3.22Hz$ for Mach 0.52. The change in lift force depends on the frequencies of pitch motion, that can be seen in Fig. 4, where the pitch frequency for Mach 0.38 is $6.92Hz$ and for Mach 0.52 is $3.33Hz$, very similar with the frequencies of the lift variation. Also, there is a considerable variation near the instant of 3.55 seconds for Mach 0.52, this instant of time is better analyzed with Figure 13.

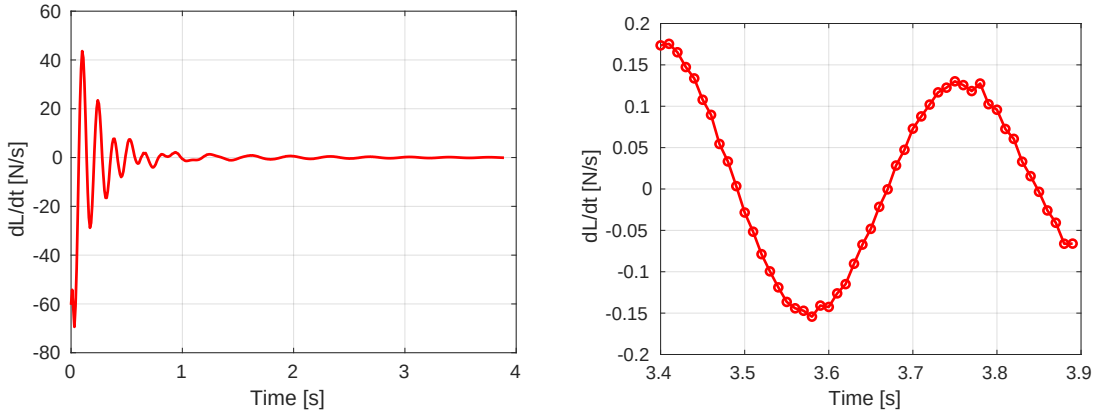

(a) (b) Zoom

Figure 11. Lift variation over time for Mach 0.38.

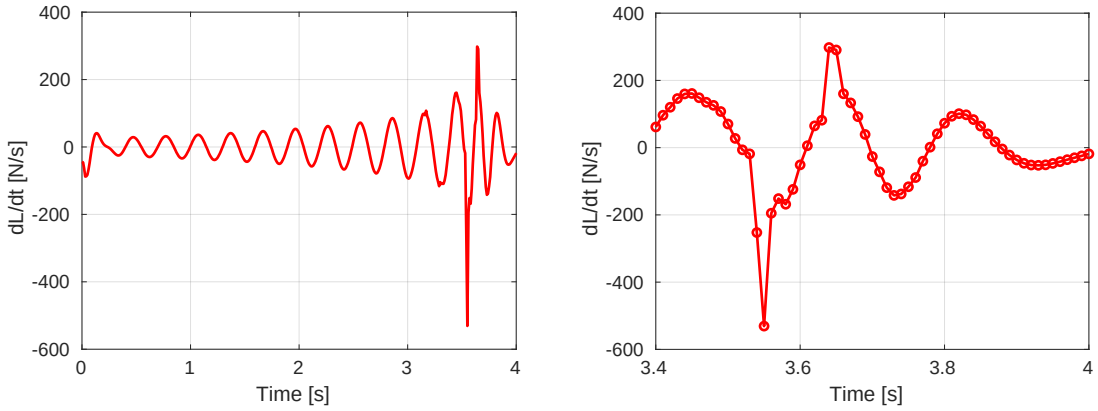

(a) (b) Zoom

Figure 12. Lift variation over time for Mach 0.52.

Figure 13 shows a comparison between the Mach number field obtained using *Paraview* and the aerodynamic force distribution on the airfoil surface for Mach 0.52 at the instant of $3.55s$. The variation shown by Fig. 12 at this instant of time is due to an aerodynamic shock, that can be noted in Fig. 13(a). The red region presents a sudden change from supersonic flow ($Ma > 1.0$) to subsonic flow ($Ma < 1.0$). Moreover, it can be seen that the methodology used to obtain the aerodynamic force is efficient, once the stagnation point computed appears at about the same location. And the high velocity region (low pressure) is well captured, once the aerodynamic forces in this location are low.

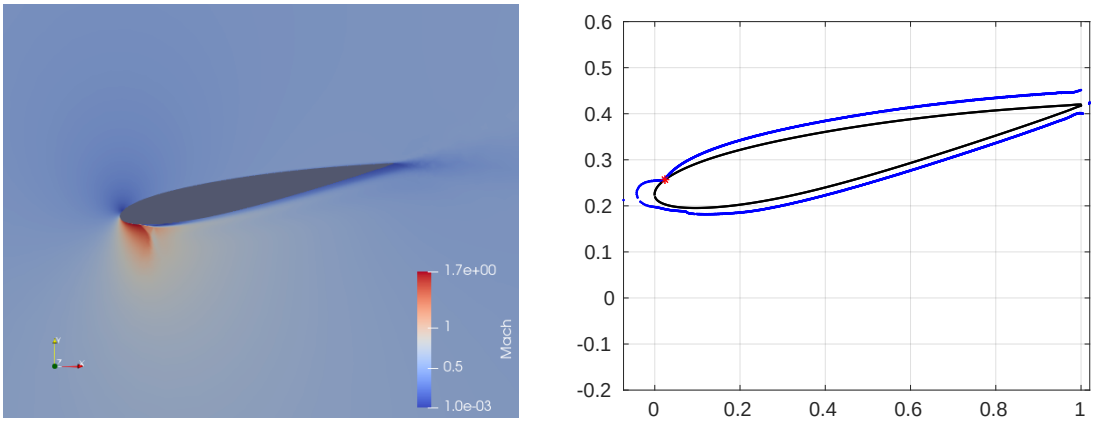

(a) (b) Zoom

Figure 13. Comparison between Mach number field and aerodynamic force distribution for Mach 0.52 at $3.55s$.

4. CONCLUSIONS

The present article introduced a strategy to evaluate the results of CFD-based solution to obtain the distribution of aerodynamic forces on an airfoil surface. The magnitude of the lift force is obtained by considering the mean pressure between two adjacent grid points and the distance between them, the direction of the lift force vector is obtained considering the decomposition of the force normal to the airfoil surface in the vertical direction. The pressure values are computed through the CFD software SU2. The airfoil pitch and plunge motion are presented in time and frequencies domains and two flow conditions are analyzed (stable and unstable).

The results show that the lift force is closely related with the pitch motion, and the stagnation point position with the plunge motion. Moreover, it can be seen that the variation of aerodynamic forces on the airfoil surface is minimal for the Mach number 0.38, but it is important for Mach number 0.52, mainly because there is the influence of aerodynamic shock. The methodology used to obtain the aerodynamic force is efficient, once the results obtained are similar with those obtained by using the post-processing software *Paraview*. Further investigations can be carried out to characterize the flutter phenomenon, and they may contribute to better evaluate the increasing amplitudes of motion. In this sense, an output-only identification method is a good topic for complementary studies in this field.

5. ACKNOWLEDGEMENTS

The first and third authors thank CNPq (National Council for Scientific and Technological Development) Grant numbers 152168/2021-4 and 314151/2021-4, respectively.

6. REFERENCES

Bisplinghoff, R.L., Ashley, H. and Halfman, R.L., 1996. *Aeroelasticity*. Dover Plublications, Inc.

Das, S.K. and Roy, S., 2018. "Finite element analysis of aircraft wing using carbon fiber reinforced polymer and glass fiber reinforced polymer." *IOP Conference Series: Materials Science and Engineering*, Vol. 402, p. 012077. doi:10.1088/1757-899x/402/1/012077.

Dash, A., 2016. "CFD analysis ofWind turbine airfoil at various angles of attack". *IOSR Journal of Mechanical and Civil Engineering*, Vol. 13, No. 04, pp. 18–24. doi:10.9790/1684-1304021824.

Dowell, E.H. and Hall, K.C., 2001. "Modeling of fluid structure interaction". *Annual Review of Fluid Mechanics*, Vol. 33, No. 1, pp. 445–490. doi:10.1146/annurev.fluid.33.1.445.

Economon, T.D., Palacios, F., Copeland, S.R., Lukaczyk, T.W. and Alonso, J.J., 2016. "SU2: An open-source suite for multiphysics simulation and design". *AIAA Journal*, Vol. 54, No. 3, pp. 828–846. doi:10.2514/1.j053813.

Fonzi, N., Cavalieri, V., Gaspari, A.D. and Ricci, S., 2021. "Advances of the python–based fluid–structureinteraction capabilities included in su2". *arXiv preprint arXiv:2109.12332*.

Garrick, I.E. and Reed, W.H., 1981. "Historical development of aircraft flutter". *Journal of Aircraft*, Vol. 18, No. 11, pp. 897–912. doi:10.2514/3.57579.

Grisval, J.P. and Liauzun, C., 1999. "Application of the finite element method to aeroelasticity". *Revue Européenne des Éléments Finis*, Vol. 8, No. 5-6, pp. 553–579. doi:10.1080/12506559.1999.10511397.

Guerri, O., Hamdouni, A. and Sakout, A., 2008. "Fluid structure interaction of wind turbine airfoils". *Wind Engineering*, Vol. 32, No. 6, pp. 539–557. doi:10.1260/030952408787548875.

Gunel, O., Koc, E. and Yavuz, T., 2016. "CFD vs. XFOIL of airfoil analysis at low reynolds numbers". In *2016 IEEE International Conference on Renewable Energy Research and Applications (ICRERA)*. IEEE, Birmingham.

doi:10.1109/icrera.2016.7884411.

Koohi, R., Shahverdi, H. and Haddadpour, H., 2014. "Nonlinear aeroelastic analysis of a composite wing by finite element method". *Composite Structures*, Vol. 113, pp. 118–126. doi:10.1016/j.compstruct.2014.03.012.

Li, W., Gao, X. and Liu, H., 2021. "Efficient prediction of transonic flutter boundaries for varying mach number and angle of attack via LSTM network". *Aerospace Science and Technology*, Vol. 110, p. 106451. doi:10.1016/j.ast.2020.106451.

Menter, F., 1993. "Zonal two equation k-w turbulence models for aerodynamic flows". In *23rd Fluid Dynamics, Plasmadynamics, and Lasers Conference*. American Institute of Aeronautics and Astronautics, Sunnyvale. doi:10.2514/6.1993-2906.

Menter, F.R., 1994. "Two-equation eddy-viscosity turbulence models for engineering applications". *AIAA Journal*, Vol. 32, No. 8, pp. 1598–1605. doi:10.2514/3.12149.

Nikbay, M., Oncu, L. and Aysan, A., 2009. "Multidisciplinary code coupling for analysis and optimization of aeroelastic systems". *Journal of Aircraft*, Vol. 46, No. 6, pp. 1938–1944. doi:10.2514/1.41491.

Peruru, S.P. and Abbisetti, S.B., 2017. "Design and finite element analysis of aircraft wing using ribs and spars". *International Research Journal of Engineering and Technology*.

Ryabinin, A. and Kuzmin, A., 2020. "Transonic flow simulation in a bent channel using SU2 software". In *2020 Ivannikov Ispras Open Conference (ISPRAS)*. IEEE. doi:10.1109/ispras51486.2020.00034.

Şahin, İ. and Acir, A., 2015. "Numerical and experimental investigations of lift and drag performances of NACA 0015 wind turbine airfoil". *International Journal of Materials, Mechanics and Manufacturing*, Vol. 3, No. 1, pp. 22–25. doi:10.7763/ijmmm.2015.v3.159.

Sanchez, R., Kline, H.L., Thomas, D., Variyar, A., Righi, M., Economon, T., Alonso, J.J., Palacios, R., Dimitriadis, G. and Terrapon, V., 2016. "Assessment of the fluid-structure interaction capabilities for aeronautical applications of the open-source solver su2". *VII European Congress on Computational Methods in Applied Sciences and Engineering*.

SU2 Foundation, 2022. "SU2 official website". URL `https://su2code.github.io/`.

Teixeira, P. and Awruch, A., 2005. "Numerical simulation of fluid–structure interaction using the finite element method". *Computers & Fluids*, Vol. 34, No. 2, pp. 249–273. doi:10.1016/j.compfluid.2004.03.006.

Zaide, A. and Raveh, D., 2006. "Numerical simulation and reduced-order modeling of airfoil gust response". *AIAA Journal*, Vol. 44, No. 8, pp. 1826–1834. doi:10.2514/1.16995.

7. RESPONSIBILITY NOTICE

The authors are solely responsible for the printed material included in this paper.